

Enhanced Long-term Stability of Organic Electrode materials by a Trap Filler Strategy

Manlin Zhao^a, Huanhuan Zhang^{*a}, and Yuguang Ma^{*a,b}

^aState Key Laboratory of Luminescent Materials and Devices, Institute of Polymer Optoelectronic Materials and Devices, South China University of Technology, No. 381 Wushan Road, Tianhe District, Guangzhou, 510640, P. R. China.

^bGuangdong Provincial Key Laboratory of Luminescence from Molecular Aggregates, South China University of Technology, No. 381 Wushan Road, Tianhe District, Guangzhou, 510640, P. R. China.

E-mail: hh_zhang@outlook.com; ygma@scut.edu.cn.

Electrochemical behaviors of AQCz, BthCz and PBICz.

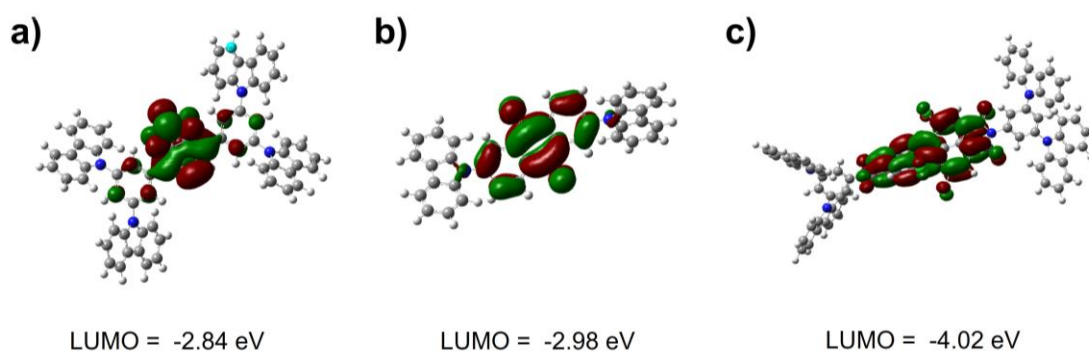


Figure S1. Frontier molecular orbitals of a) BthCz, b) AQCz and c) PBICz. Optimization of the chemical structures was performed with Gaussian software with the PM6-D3 method. Calculations of the frontier molecular orbitals were also performed by Gaussian using density functional theory [B3PW91/6-31g(d)].

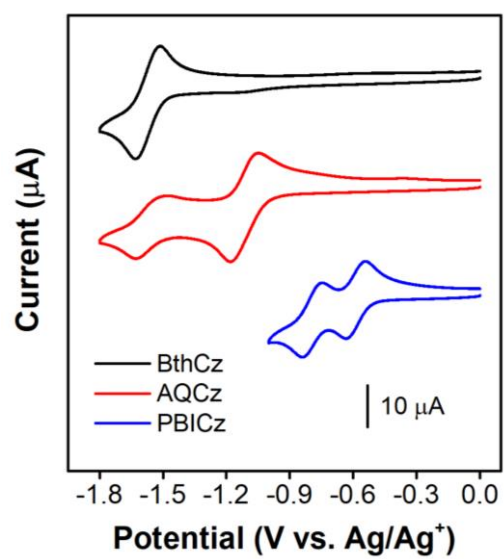


Figure S2. CV curves of BthCz, AQCz and PBICz in dichloromethane electrolyte.

Glassy carbon and platinum disk were chosen as working electrode and counter electrode, respectively. The monomer concentrations of AQCz, BthCz and PBICz were 2.5×10^{-4} , 2.5×10^{-4} , and 7.5×10^{-5} M, respectively. AQCz EP film was generated in dichloromethane with the potential window of -0.5 ~ 1.40 V, the scan rate of 100 mV s^{-1} and the scan cycles of 15. BthCz EP film was generated in mixed solvents (dichloromethane: acetonitrile = 3:2 V:V) with the potential window of -0.5 ~ 1.20 V, the scan rate of 100 mV s^{-1} and the scan cycles of 8. PBICz EP film was generated in mixed solvents (dichloromethane: acetonitrile = 3:2 V:V) with the potential window of 0 ~ 1.15 V, the scan rate of 100 mV s^{-1} and the scan cycles of 20. All the EP films above were washed with dichloromethane and acetonitrile, respectively after EP and dried at 120°C under oven for 1 h to remove residual water.

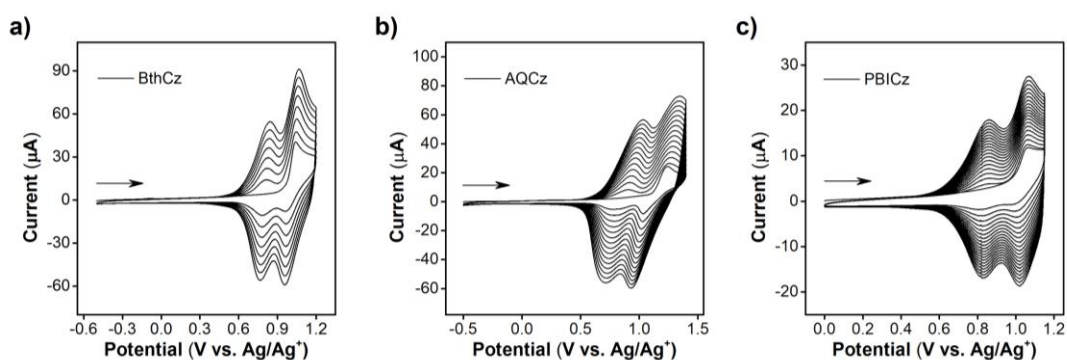


Figure S3. CV curves of a) BthCz, b) AQCz and c) PBICz during EP.

Electrochemical behaviors of acetonitrile solvent with different contents of water or oxygen.

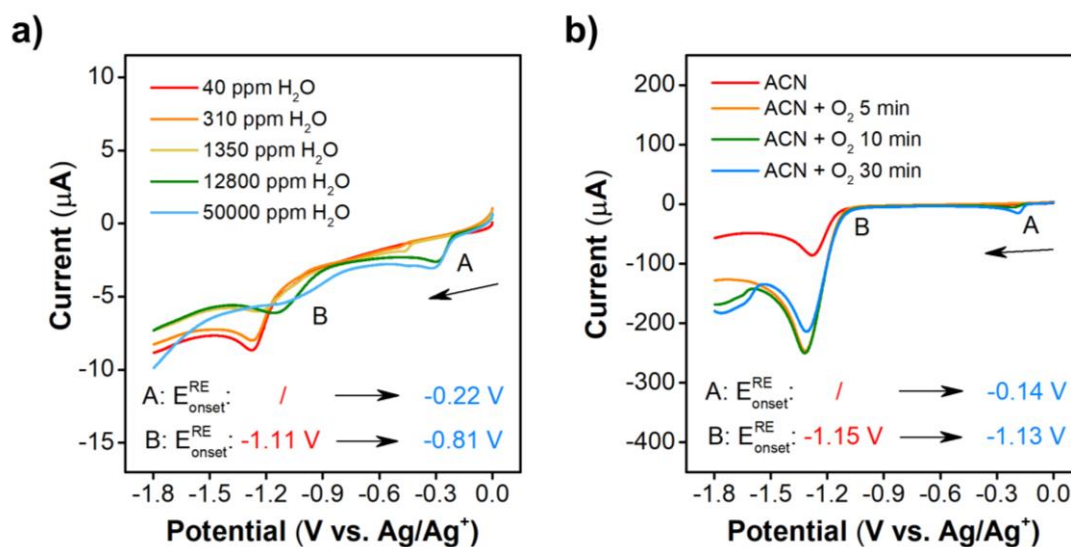


Figure S4. LSV curves of acetonitrile electrolytes containing a) different contents of water or b) oxygen (scan rate: 100 mV s^{-1}).

Electrochemical behaviors of DMC.

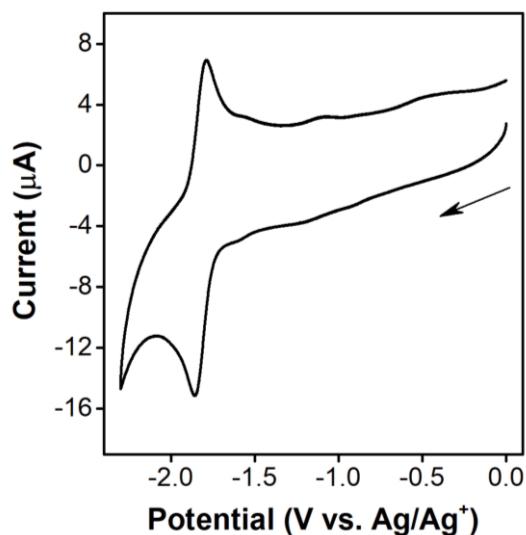


Figure S5. CV curve of DMC ($2.5 \times 10^{-4} \text{ M}$) in dichloromethane.

CV curves of BthCz, AQCz and PBICz EP films with different contents of water with/without DMC.

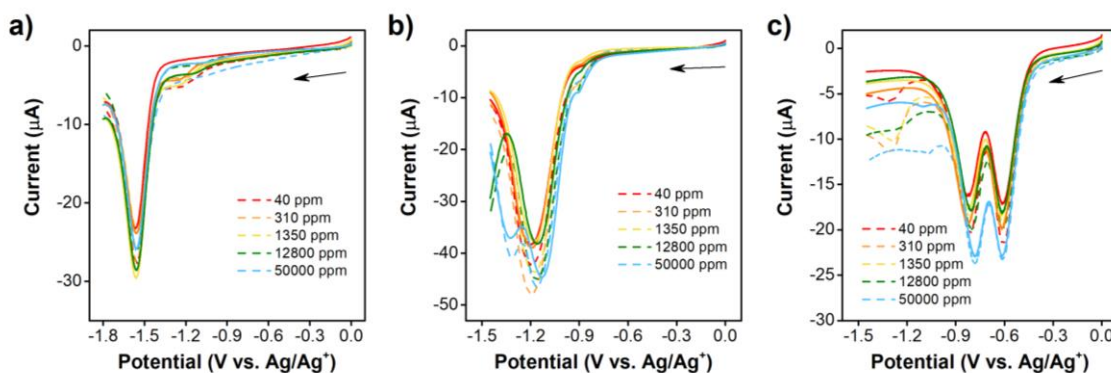


Figure S6. CV curve of a) BthCz, b) AQCz and c) PBICz EP films with different contents of water with (solid line) or without (dash line) DMC.

CV curves of BthCz and AQCz EP films with different contents of DMC.

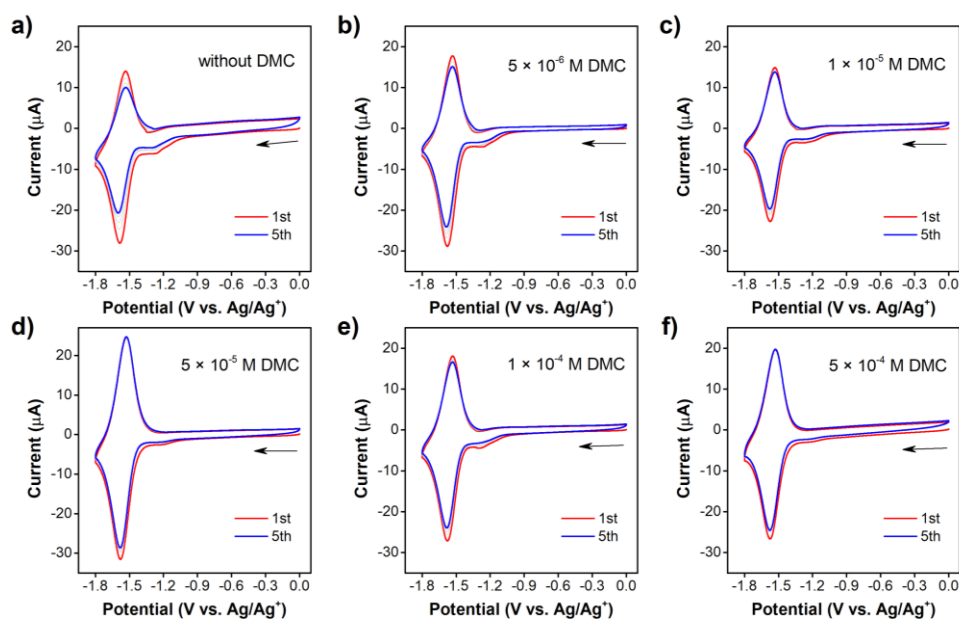


Figure S7. CV curves of BthCz EP films in a) acetonitrile electrolyte and electrolytes containing b) - f) 5×10^{-6} , 1×10^{-5} , 5×10^{-5} , 1×10^{-4} and 5×10^{-4} M DMC (potential window: 0 ~ -1.80 V, scan rate: 50 mV s^{-1}).

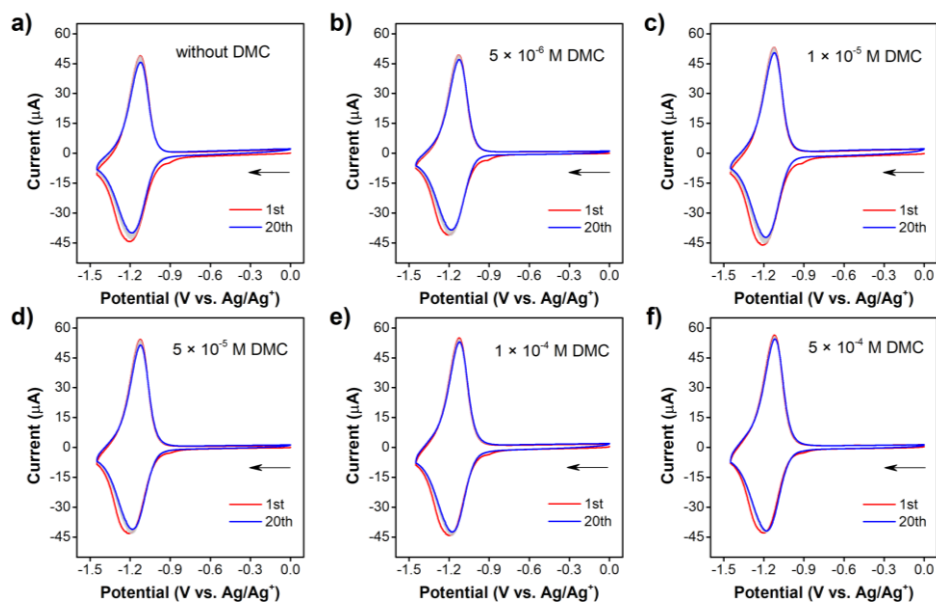


Figure S8. CV curves of AQCz EP films in a) acetonitrile electrolyte and electrolytes containing b) - f) 5×10^{-6} , 1×10^{-5} , 5×10^{-5} , 1×10^{-4} and 5×10^{-4} M DMC (potential window: 0 ~ -1.45 V, scan rate: 50 mV s^{-1}).

Table S1. Charge Retention of BthCz and AQCz EP Films in Electrolytes Containing Different Contents of DMC

	BthCz EP films (5 cycles)	AQCz EP films (20 cycles)
acetonitrile electrolyte	80.5%	86.3%
with 5×10^{-6} M DMC	84.1%	91.0%
with 1×10^{-5} M DMC	88.7%	88.7%
with 5×10^{-5} M DMC	90.8%	92.8%
with 1×10^{-4} M DMC	89.2%	94.5%
with 5×10^{-4} M DMC	91.7%	95.7%

Stability of PBICz EP film in DMC electrolyte.

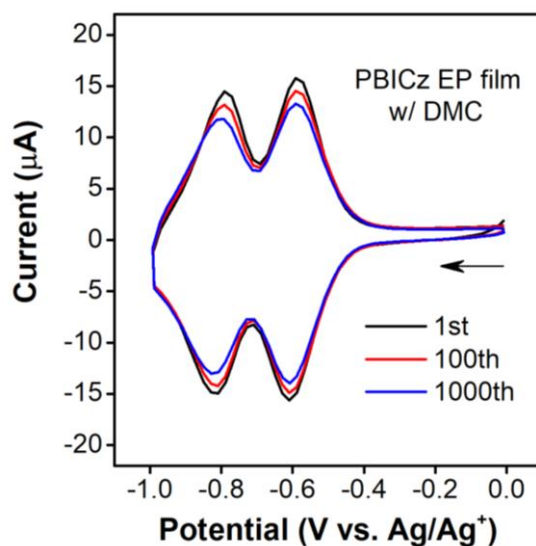


Figure S9. CV curves of PBICz EP film in electrolyte containing DMC (potential window: 0 ~ -1.0 V, scan rate: 100 mV s⁻¹).

SEM images of BthCz, AQCz and PBICz EP films

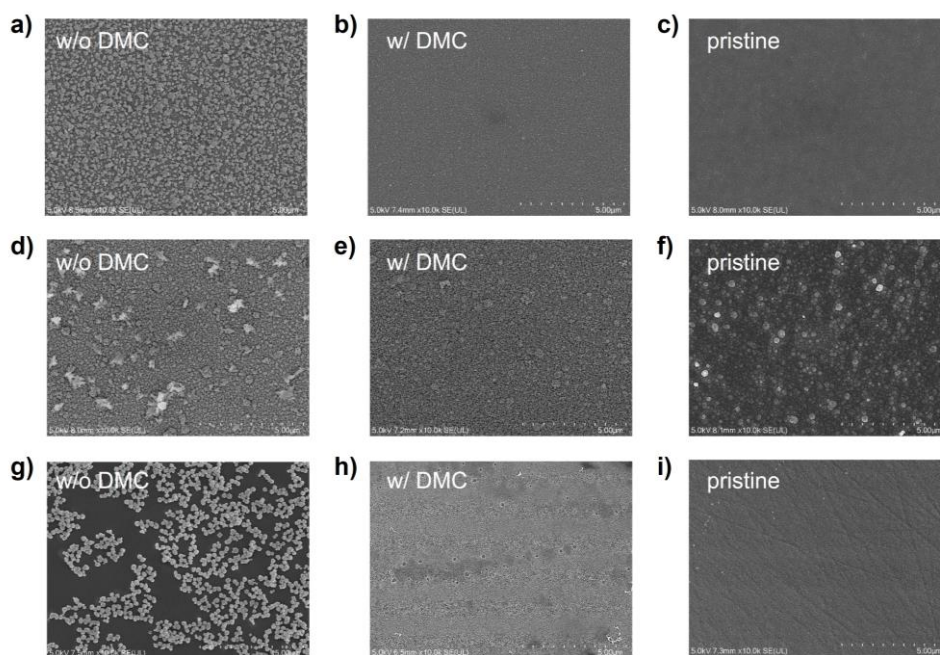


Figure S10. SEM images of a) BthCz, d) AQCz and g) PBICz EP films after multiple cycles (400, 970 and 1000 cycles, respectively) in blank acetonitrile electrolyte; SEM images of b) BthCz, e) AQCz and h) PBICz EP films after multiple cycles in 5×10^{-4} M DMC electrolyte; SEM images of c) BthCz, f) AQCz and i) PBICz EP films of pristine.

***In situ* UV-vis spectroelectrochemistry of EP films.**

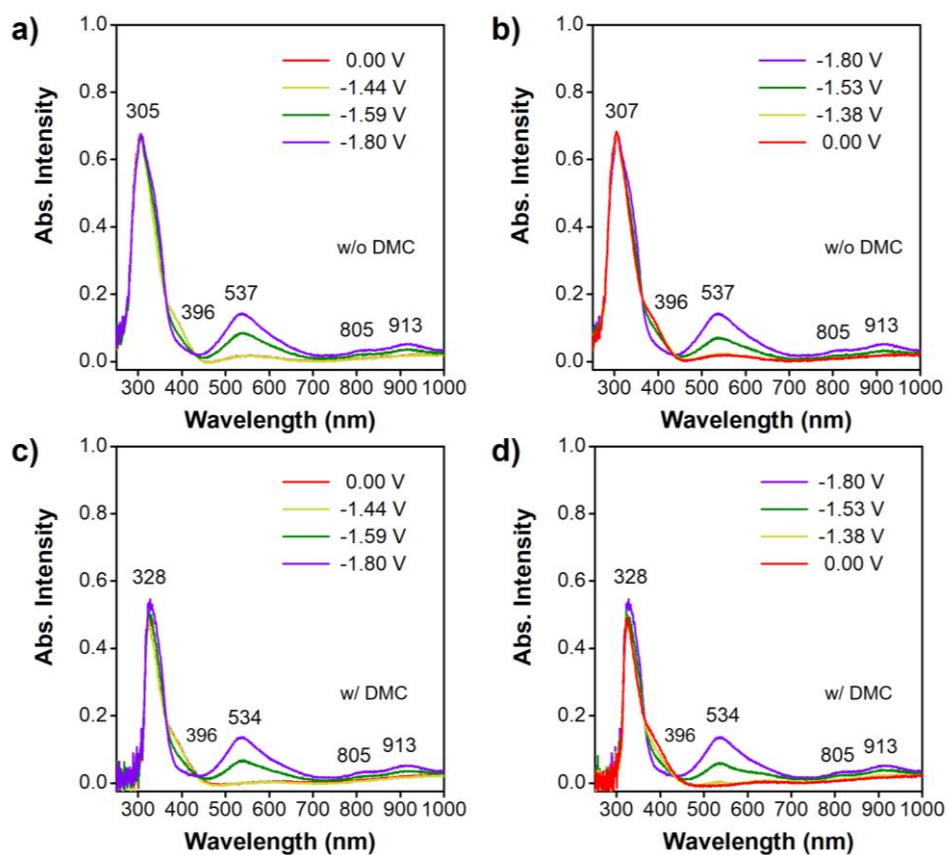


Figure S11. The first cycle of doping (left column, from 0 to -1.80 V) and dedoping (right column, from -1.80 to 0 V) process of BthCz EP films in a), b) acetonitrile electrolyte and c), d) electrolyte containing 5×10^{-4} M DMC (potential window: 0 ~ -1.80 V, scan rate: 50 mV s⁻¹).

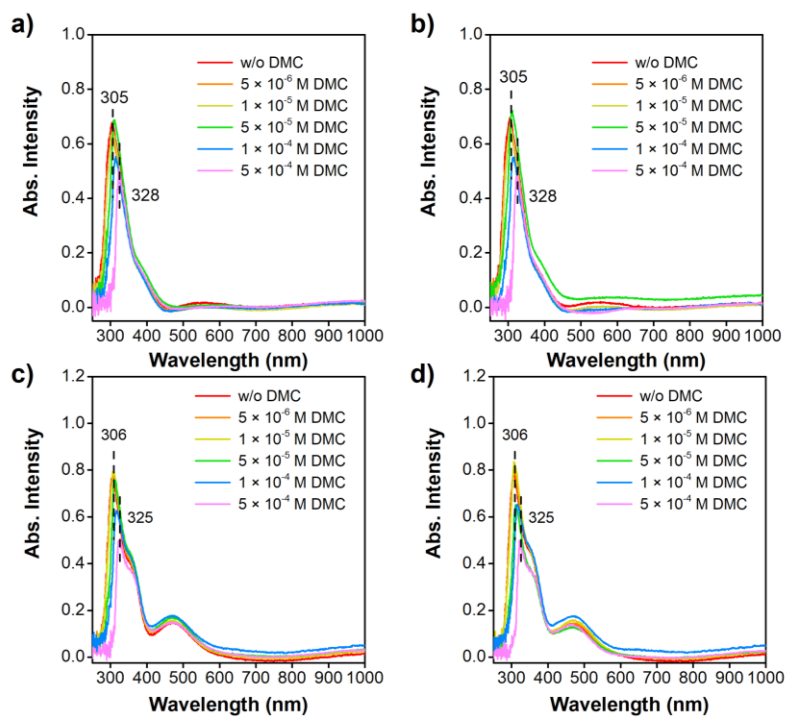


Figure S12. *In situ* UV-vis spectra of initial state (left column) and after 5 cycles (right column) of a), b) BthCz and c), d) AQCz EP films in electrolytes with different concentrations of DMC.

UV-vis spectra of three electrode materials and DMC

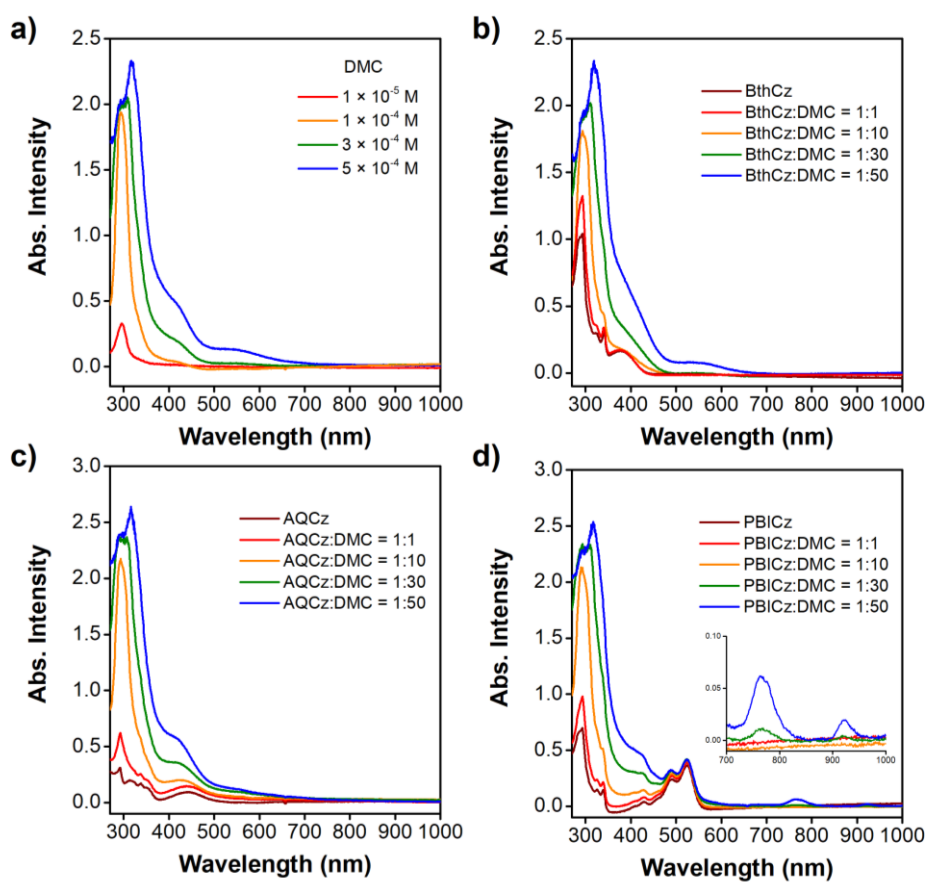


Figure S13. UV-vis spectra of different concentration of a) DMC, b) BthCz monomer with DMC, c) AQCz monomer with DMC and d) PBICz monomer with DMC (The concentration of BthCz, AQCz and PBICz was 1×10^{-5} M, and dichloromethane was chosen as solvent) .

Results of electrolyte containing 5×10^{-4} M DMC with different contents of water.

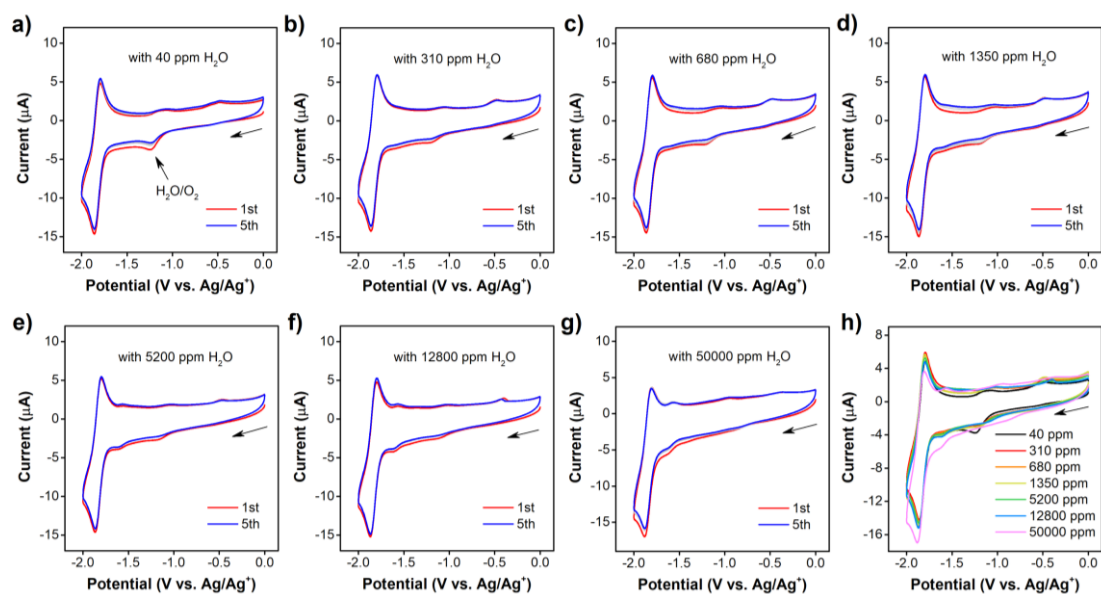


Figure S14. CV curves of 5×10^{-4} M DMC with a) 40, b) 310, c) 680, d) 1350, e) 5200 f) 12800 and g) 50000 ppm water. h) The first cycle of CV curves of 5×10^{-4} M DMC with different contents of water (potential window: 0 ~ -2.0 V, scan rate: 100 mV s^{-1}).

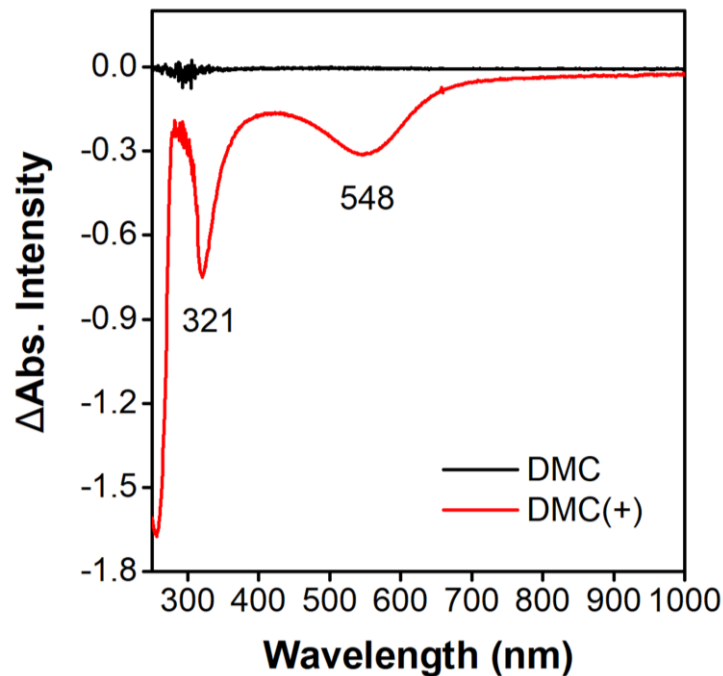


Figure S15. UV-vis spectra of 5×10^{-4} M DMC(+) solvent with the absorbance of 5×10^{-4} M DMC as baseline.



Figure S16. Photo image of 5×10^{-4} M DMC(+).

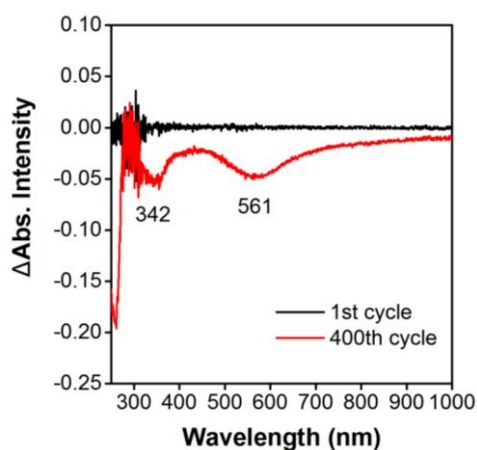


Figure S17. *In situ* spectroelectrochemistry of 5×10^{-4} M DMC, with the initial absorbance as baseline (potential window: 0 ~ -2.0 V, scan rate: 100 mV s^{-1}).

The monomer concentration of DMC and DMC(+) was 5×10^{-4} M, and acetonitrile was chosen as solvent.

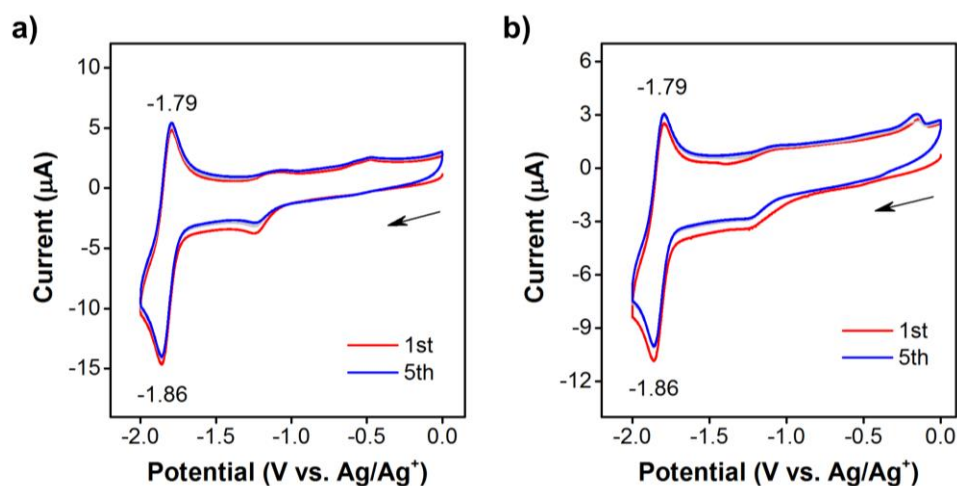


Figure S18. CV curves of a) DMC and b) DMC(+) (potential window: 0 ~ -2.0 V, scan rate: 100 mV s^{-1}).